Full text open access online (Since 2001)

PRINT: ISSN 0972-3757 ONLINE: ISSN 2456-6330
Int J Hum Genet, 24(2): 170-182 (2024)
DOI: 10.31901/24566322.2024/24.02.881

Participation of the LINC00174/miR-144-3p/Nrf2 Pathway in Oral Tongue Squamous Cell Carcinoma Cells

Huaiguang Chang[1, 2, 3], Tingting Jiang[4], Taixing Cui[3], Liang Kou[1], Xinchen Yu[1] and Lei Zhang[1,*]

[1] Department of Stomatology, Ningbo College of Health Sciences, Ningbo 315100, Zhejiang Province, China
[2] Ningbo Oral Health Research Institute, Ningbo 315100, Zhejiang Province, China
[3] Department of Prosthodontics, Yinzhou Stomatology Hospital, Ningbo 315100, Zhejiang Province, China
[4] Department of Orthodontics, Yinzhou Stomatology Hospital, Ningbo 315100, Zhejiang Province, China

KEYWORDS Carcinoma. Cell. Expression. Long Non-coding RNA. microRNA

ABSTRACT This study aims to examine how long non-coding ribonucleic acid 00174 (LINC00174) influences micro RNA (miR)-144-3p/nuclear factor erythroid 2-related factor 2 (Nrf2) signalling pathway, as well as its effects on cell proliferation, invasion, apoptosis, and transformation in oral tongue squamous cell cancer. Si-Nrf2, si-LINC00174, miR-144-3p inhibitor, miR-144-3p inhibitor + si-LINC00174, miR-144-3p inhibitor + si-Nrf2, and corresponding control were transfected into SCC-9 cells. The relationships among miR-144-3p, LINC00174, and Nrf2 were established. Reversing the miR-144-3p suppression could restore the diminished migratory, proliferative, and invasive capabilities of SCC-9 cells resulting from the inhibition of LINC00174 and Nrf2. Furthermore, it decreased the levels of Vimentin and Snail expression while enhancing E-cadherin expression level ($P<0.05$). In conclusion, as for oral tongue squamous cell cancer, LINC00174 at an excessive expression level in SCC-9 cells has the potential to take advantage of the miR-144-3p/Nrf2 signalling pathway to boost the migratory plus invasive capabilities, while inhibiting apoptosis of cells.

INTRODUCTION

In 1975, oral cancer was recognised as a unique clinical disease (Mneimneh et al. 2021). Since then, this cancer has attracted widespread attention. Bray et al. (2018) reported that there were 354,864 newly identified instances of oral cancer, resulting in 177,384 deaths. Additionally, Mascitti et al. (2020) stated that oral tongue squamous cell cancer (OTSCC) accounts for over 90 percent of all oral malignancies. OTSCC mainly exists in the tongue, gums, hard palate, and floor of the mouth (De Araújo et al. 2022). Currently, the general outlook for patients with OTSCC is still unsatisfactory because of the recurrence of the disease in the local area and its spread to other parts of the body (Adeoye et al. 2021). Hence, investigating the molecular mechanism underlying the growth dominance of OTSCC cells may provide a novel therapeutic target.

According to Li et al. (2021a), lncRNAs, which are longer than 200 nt, lack protein-coding sequences. Recent verification has shown a close association between lncRNAs and kinases, receptors, transcription factors, and other signal transmitters through diverse signalling pathways (Lampropoulou et al. 2021). In clinical practice, the abnormally expressed lncRNAs in the cancer tissues of patients often lead to poor prognosis besides metastasis (Liu et al. 2021). The role of LINC00174 as a reservoir for different microRNAs (miRNAs) in regulating the growth, programmed cell death, and movement of glioma cells has been corroborated by Li et al. (2020). Moreover, it has been combined with miRNAs to inhibit numerous forms of cancer (Wang et al. 2020; Ma et al. 2021; Cheng et al. 2022). Pitifully, there has been limited investigation into LINC00174's role in OTSCC thus far.

MiRNAs control the proliferation, apoptosis, invasion, migration, other phenotypes, and diverse cellular characteristics by virtue of the interaction with the 3'-UTR of their target genes (Kazmierczak and Hydbring 2021). In terms of colorectal cancer cells, for example, miR-144-3p targets ZEB1/2 to obstruct the progression, invasion, and transition from epithelial to mesenchymal state (EMT) (Li et al. 2021c). Cao et al. (2020) discovered that the up-

*Address for correspondence:
Lei Zhang
E-mail: zhangleinchs@csc-edu.cn

regulation of PTEN expression promotes the advancement of thyroid tumours. As stated by Li et al. (2021b), inhibition of CEP55 expression hindered non-small cell lung cancer from progression. Furthermore, miR-144-3p selectively aimed at Nrf2, a nuclear factor associated with erythroid 2, leading to successful inhibition of its expression, according to Zhao et al. (2021). Nevertheless, it remains uncertain if the advancement of OTSCC is influenced by LINC00174 via the modulating effect of miR-144-3p on Nrf2 expression.

Objectives

The present study is intended to examine the LINC00174/miR-144-3p/Nrf2 pathway under OTSCC from the aspects of possible molecular mechanism together with expression, aiming at laying a theoretical foundation for treating OTSCC in clinic.

MATERIAL AND METHODS

Gathering of Clinical Specimens

Before use, fresh tissues from 38 patients with OTSCC (n=38) along with corresponding normal paracancerous tissues (n=38) were subjected to -80°C preservation. The research ethics committee of the hospital granted approval for the present study, while all participants gave their consent by signing the informed consent form after being adequately informed of the experiment.

Culture and Transfections of Cells

The Cell Bank at Shanghai Institute of Biochemistry and Cell Biology, CAS (China) supplied HIOEC cell line and OTSCC cell lines (SCC-25, SCC-4, CAL27, and SCC-9), as well as the corresponding culture media. SCC-9 cells underwent transfection with Lipofectamine 2000 reagent supplied by Thermo Fisher Scientific (USA). After that, various groups, such as si-NC group (negative control for small interfering), inhibitor-NC group (negative control for miR-144-3p-inhibitor), si-Nrf2 + inhibitor group (si-Nrf2 + miR-144-3p-inhibitor), inhibitor group (miR-144-3p-inhibitor), si-Inc group (si-LINC00174), si-Inc + inhibitor group (si-LINC00174 + miR-144-3p-inhibitor), and si-Nrf2 group were set up for the cells.

Colony Formation Assay

Following transfection, a 6-well plate was employed for gathering and placing the SCC-9 cells (500 cells/well in concentration). Then the colonies underwent staining using 0.1 percent crystal violet subsequent to paraformaldehyde (4%) treatment in order to assess the rate of colony formation.

Xenotransplantation Procedure

After successfully transfecting si-NC and si-Inc, nude mice (BALB/c, male, n=5) aged 6 weeks (Shanghai Laboratory Animal Research Center, China) were injected with SCC-9 cells. Weekly measurements were taken of the tumour's dimensions using callipers, and its volume was calculated by multiplying the length, the width squared, and 0.52. Following a period of 5 weeks from inoculation, each mouse was euthanised. Next, the tumour masses were surgically removed in order to analyse their weight afterwards. The animal experiments were implemented by the hospital *as per* the guidelines specified in the *Guide for the Care and Use of Laboratory Animals*, with an approval obtained from the Animal Care and Use Committee.

Extraction of Nucleic Acids plus Quantitative Reverse Transcription-Polymerase Chain Reaction (qRT-PCR)

RNAiso Plus and RNAiso for Small RNA (TaKaRa, Japan) were adopted to separate miRNA as well as total RNA, and the reverse transcription was carried out in line with the PrimeScrip RT reagent kit (Takara, Japan) instructions. Afterwards, TB Green Premix Ex Taq II (Takara, Japan) was applied to exert qRT-PCR through an Mx3000p real-time PCR system (Agilent, USA). The process included a 3-minute preliminary pre-denaturation phase at 95°C, prior to (15 seconds of 95°C denaturation and 1 minute of 60°C annealing) × 40 rounds, along with a 7-minute concluding extension at 68°C. To calculate the results, the $2^{-\Delta\Delta Ct}$ approach was utilised, where the controls of Glyceraldehyde-3-phosphate dehydrogenase (GAPDH) for mRNA plus U6 for miRNA were adopted.

CCK-8 Assay Used for Counting Cells

Following a 24-hour transfection period, the SCC-9 cells, which were experiencing optimal growth, were gathered to form a solution of sepa-

rate cells (1×10^4 /mL) and subsequently inserted into a 96-well plate. After culture, CCK-8 solution (volume: 10 μL) was added for treatment of every well of cells for 1 hour at 0, 24, 48, and 72 hours of incubation. Afterward, a microplate reader was used to examine each well at the 450 nm wavelength to obtain the optical density (OD_{450}).

Target Gene Prediction

The website miRDB (http //mirdb.org/) and starBase v2.0 (http //starbase.sysu.edu.cn/starbase2) were employed to make predictions about the target gene and target miRNA for miR-144-3p and LINC00174, respectively.

Dual-luciferase Reporter Gene Assay

The DNA of the human genome was utilised to enhance and clone the sequences located in the 3'-UTR of LINC00174 and Nrf2 into pGL3 luciferase reporter vectors. A change happened in the presumed miR-144-3p binding location. Afterwards, SCC-9 cells underwent co-transfection with Nrf2 vector and LINC00174 vector, which contained the 3'-UTRs of wild-type/mutant (WT/MUT). Furthermore, transfection also involved the inclusion of control mimic and miR-144-3p mimic. Afterwards, the luciferase activity was acquired and then standardised.

Investigation of RNA Interactions *via* RNA Immunoprecipitation (RIP) Assay

An RNA-binding protein immunoprecipitation kit (Magna RIP™) provided by Sigma-Aldrich (USA) was utilised to implement the RIP experiment. RIP buffer was used to lyse the SCC-9 cells. Subsequently, the mixture of supernatant and proteins was combined with A/G magnetic beads that were linked to antibodies against IgG plus Ago2 (Abcam, USA). Finally, immunoprecipitated RNAs were acquired through the interaction of the samples with proteinase K, then extracting the RNAs and subsequently conducting qRT-PCR to detect the levels of LINC00174 and miR-144-3p.

Western Blotting

The transfected cells were selected to obtain proteins which were then moved to RIPA lysis buffer (Thermo Fisher Scientific, USA). Afterwards, Thermo Fisher Scientific (USA) supplied the BCA protein assay kit for the determination of protein concentration. Subsequently, protein concentration was achieved in a gel containing 5 percent concentration, followed by separation using SDS-PAGE with a 10 percent concentration. Then a PVDF membrane was applied to transfer the isolated proteins for 2 hours. Afterwards, the membrane underwent incubation at a temperature of 4°C overnight with antibodies against Nrf2, E-cadherin, B-cell lymphoma-2 (Bcl-2), Vimentin, Snail, Bcl-2-associated X protein (Bax), and GAPDH (Abcam, USA). The next day, the membrane underwent room-temperature incubation for a duration of 1 hour under supplemented secondary antibodies (Abcam, USA). Finally, LI-COR Biosciences (USA) offered an Odyssey system to analyse the results of the experiment.

Transwell Assay

To conduct the invasion experiment, SCC-9 cells were cultivated in a Transwell apparatus with a Matrigel basement membrane (Corning, USA) coating on the underside. Specifically, the cells were cultivated in a medium without serum, whereas the lower section of the 24-well plate in the Transwell chamber was supplied with the FBS (20 %)-containing medium solution (0.6 mL in volume). Around 48 hours later, crystal violet staining was carried out on the cells migrating into the lower side of the membrane from the upper side. In the end, the intrusive cells were tallied in five fields chosen at random using a light microscope from Olympus (Japan).

Assessment of Healing Process of Wounds

Single-layer cells cultured in the 12-well plate with 100 percent confluence were scraped using a 20 μL pipette tip. Then the cell fragments in the plate were gently removed by washing. At 0 hours, scratches were made on the cells, followed by cell culture with medium containing no FBS. The cells were examined using a microscope at 0 and 24 hours after being cultured. The formula listed below was applied to calculate the migration rate:

Cell migration rate (%) = (initial scratch distance - scratch distance at 24 hours) / initial scratch distance × 100 percent.

Statistical Analysis

The data was analysed using Prism7 software from GraphPad (USA), and presented as the mean ± standard deviation (x ± s). The connections among the manifestations of LINC00174, miR-144-3p, and Nrf2 were evaluated by means of Pearson's examination. The comparison of data between two groups and among multiple groups was realized using independent samples t-test and one-way analysis of variance, respectively. A difference of statistical significance was denoted with $P<0.05$.

RESULTS

LINC00174 Overexpression in Cell Lines besides Tissues of OTSCC in Human Beings

Among the lncRNAs presenting differential expressions identified through second-generation sequencing, LINC00174 was selected, with its expressions verified in OTSCC tissues and non-OTSCC tissues. For the purpose of appraising how LINC00174 modulates OTSCC progression in human body, the researchers performed qRT-PCR to initially analyse LINC00174 expression in totally 38 cases of OTSCC tissues obtained from patients through. OTSCC tissues exhibited significantly increased LINC00174 at the expression level compared to the corresponding non-OTSCC tissues (Fig. 1A). Following that, LINC00174 proportional levels in HIOEC plus OTSCC cell lines (SCC-25, SCC-4, CAL27, SCC-9, etc.) were identified *via* qRT-PCR. In Figure 1B, by contrast with that in HIOEC cells at the expression level, prominently raised LINC00174 was observed in SCC-25, CAL27, SCC-4, and SCC-9 cells ($P<0.01$). SCC-9 cells had the highest level. As a result, SCC-9 cells were used in subsequent experiments. In addition, the cytoplasm displayed a greater amount of LINC00174 in comparison to the nucleus (Fig. 1C). Taken together, high LINC00174 expression probably acts as a vital player in OTSCC.

Functions of Inhibiting LINC00174 in OTSCC Cell Propagation, Invasion, Movement, Apoptosis, as well as EMT

The siRNA method was utilised to inhibit the expression of LINC00174 to examine its effect on SCC-9 cells. Subsequently, si-NC and si-Inc were used for cell transfection. According to Figure 2A, LINC00174 displayed a notably lowered expression level subsequent to si-Inc transfection ($P<0.01$). Besides, SCC-9 cell proliferation was significantly reduced after LINC00174 knockdown (Fig. 2B). Furthermore, OTSCC cell growth was restrained thereby in terms of colony formation (Fig. 2C). Moreover, the inhibition of LINC00174 significantly attenuated the invasive together with migratory capability of OTSCC cells (Fig. 2D and E). Furthermore, the inhibition of LINC00174 significantly elevated the protein quantities of Bax ($P<0.01$) while

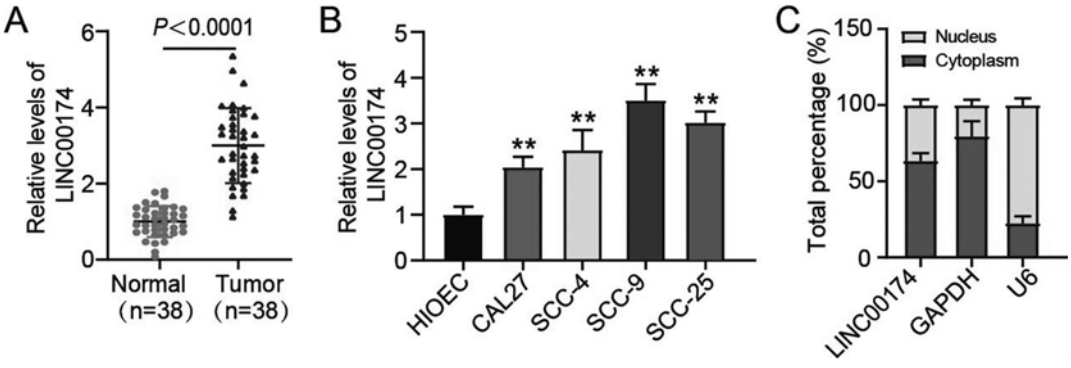

Fig. 1. Expression of LINC00174 in oral tongue squamous cell carcinoma (OTSCC) tissues and cells. A: The expression of LINC00174 in various tissues. B: LINC00174 expression in cell lines. C: Expression of C LINC00174 in the cytoplasm and nucleus of SCC-9 cells. **P<0.01 vs. HIOEC cells

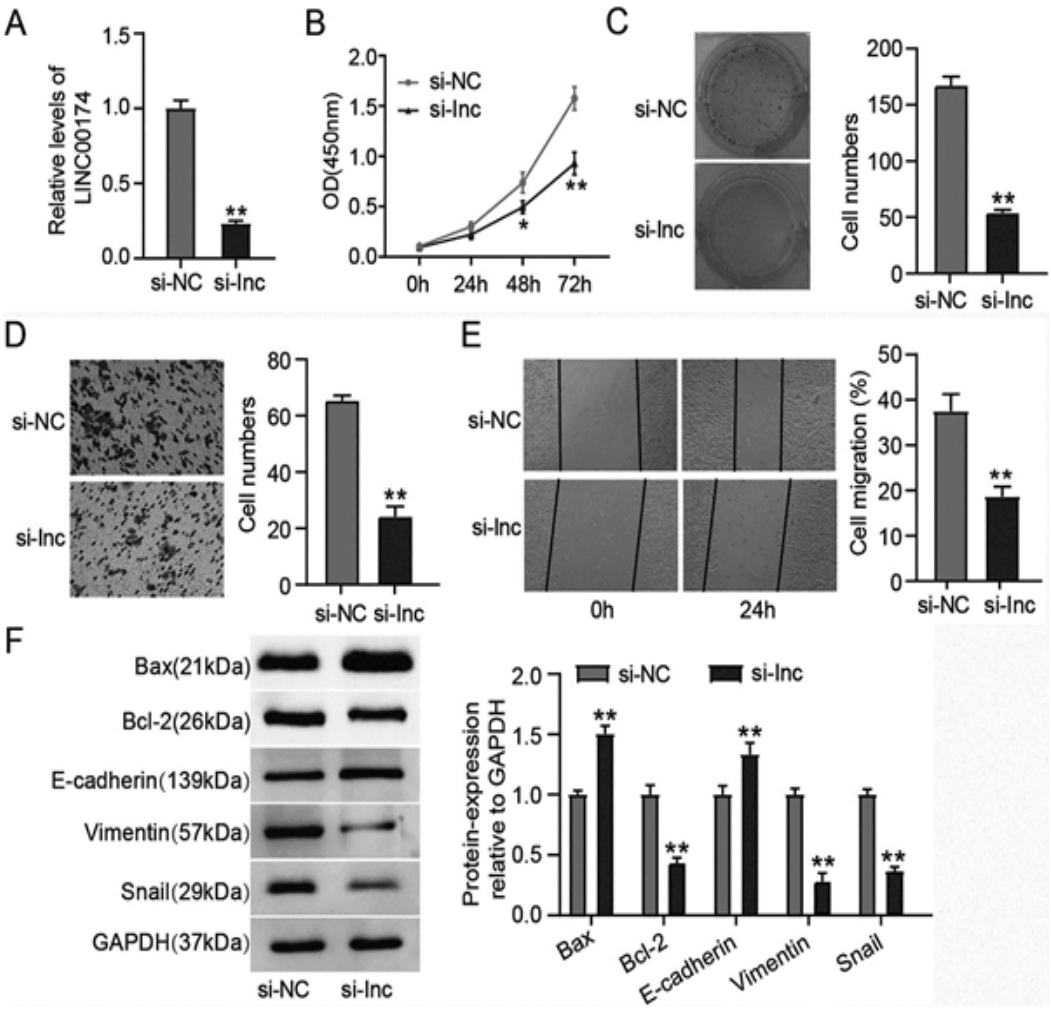

Fig. 2. Silencing of LINC00174 inhibits the growth, infiltration, and movement while enhancing the programmed cell death and epithelial-mesenchymal transition of OTSCC cells. A: An examination of the impact of reducing LINC00174 on SCC-9 cells following transfection. B: Cell viability was assessed using the CCK-8 assay. C: Cell colony formation rate. D: Cell invasion capability observed using the Transwell assay. E: The ability of cells to migrate was assessed using a wound healing assay. F: Western blotting detected the protein expressions of Bax, Bcl-2, E-cadherin, Vimentin, and Snail. si-Inc: si-LINC00174. *P<0.05 and **P<0.01 vs. si-NC group

reducing those of Bcl-2 (P<0.01), indicating that the absence of LINC00174 facilitated SCC-9 cell apoptosis. After LINC00174 was repressed, raised E-cadherin expression, along with reduced Snail plus Vimentin expressions, were detected from SCC-9 cells. These findings suggest that LINC00174 promotes the process of EMT, as depicted in Figure 2F.

Effect of Inhibiting LINC00174 on *in vivo* Tumour Development

The tumour volume was measured weekly by injecting SCC-9 cells transfected with si-NC and si-Inc to create a mouse xenotransplantation model. At 5 weeks after inoculation, the tumour was

weighed. During the second week, the difference in tumour volume compared involving the si-Inc and si-NC groups was statistically significant ($P<0.05$), and this difference became even more pronounced in the third week ($P<0.01$). Moreover, the tumour in the si-Inc group displayed a considerably decreased weight in comparison to the si-NC group (Fig. 3). In summary, the suppressed LINC00174 restricted OTSCC cell proliferation.

LINC00174 Sponged miR-144-3p

The prospective target miRNA of LINC00174 was forecast by virtue of the starBase v2.0 website (http //starbase.sysu.edu.cn/starbase2/). LINC00174 has the potential to interact with miR-144-3p (Fig. 4A). As revealed by the dual-luciferase reporter gene assay, the luciferase activity of the LINC00174-WT reporter gene in SCC-9 cells was notably reduced by upregulated miR-144-3p expression, but that of the LINC00174-MUT reporter gene was affected to a negligible extent (Fig. 4B). RIP assay was performed to validate the intrinsic interaction of miR-144-3p with LINC00174. In comparison with the anti-IgG antibody group in Figure 4C, the utilisation of the anti-Ago2 antibody resulted in evidently enhanced LINC00174 and miR-144-3p enrichment. Moreover, miR-144-3p levels in tissues and cells were determined through qRT-PCR. Tumour tissues had markedly higher miR-144-3p expression than normal tissues ($P<0.0001$, Fig. 4D). The SCC-9 cells exhibited a notable decrease in the expression ($P<0.01$, Fig. 4E). Figure 4F illustrates the inverse correlation of LINC00174 with miR-144-3p in OTSCC cells at the expression level. LINC00174 conjugated with it to regulate miR-144-3p level.

Repressing miR-144-3p Counteracted the Impact of LINC00174 Silencing on SCC-9 Cells

The process of transfection was carried out on SCC-9 cells utilising si-Inc + inhibitor, inhibitor-NC, si-NC, si-Inc, and inhibitor. Next, qPCR was conducted to verify the success of the transfection. As shown in Figure 5A, the inhibitor group exhibited notably repressed expression of miR-144-3p ($P<0.01$). The si-Inc group exhibited a notable reduction in cellular ability to proliferate, invade, form colonies, and migrate by contrast to the si-

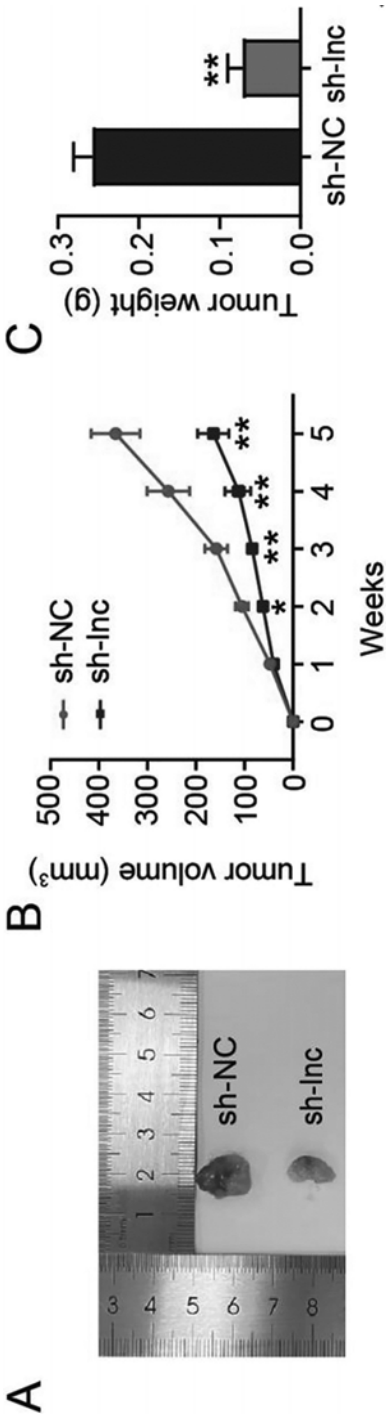

Fig. 3. In vivo, the growth of tumors is suppressed by the silencing of LINC00174. A: Tumor tissues in the mouse xenotransplantation model. B: Weekly fluctuations in tumor size. C: Weight of the tumor after 5 weeks.si-Inc: si-LINC00174. *P<0.05 and **P<0.01 vs. si-NC group

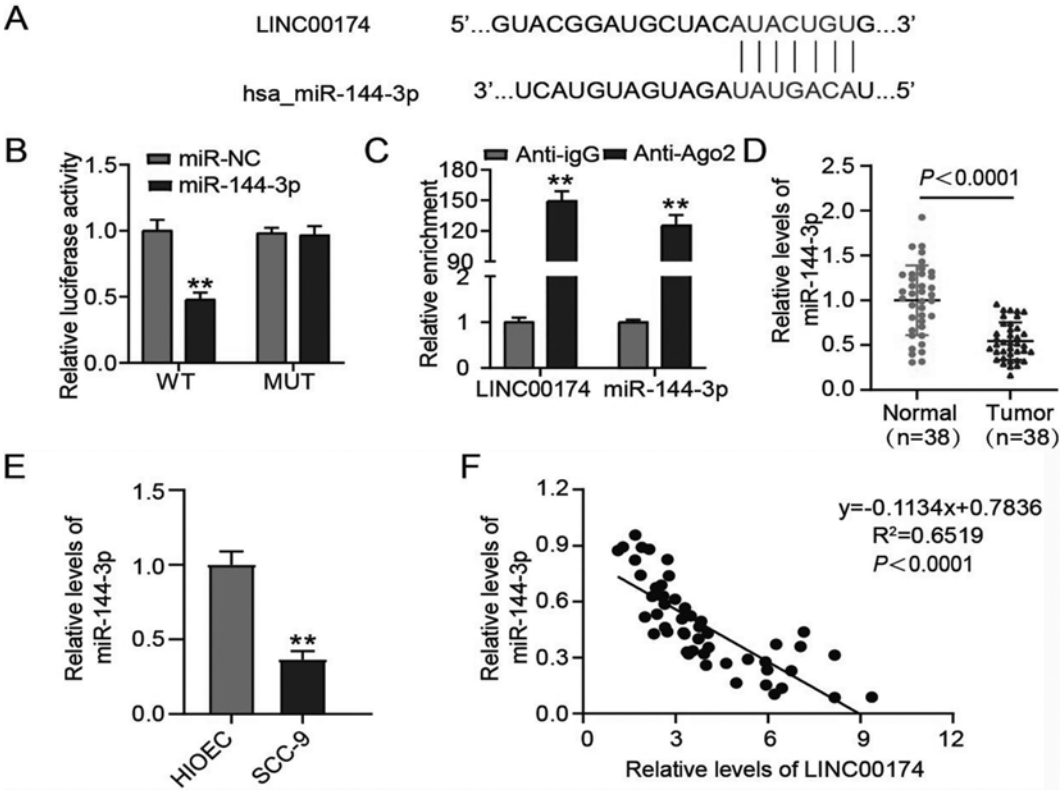

Fig. 4. The association between LINC00174 and miR-144-3p. A: A diagram illustrating the target sequence of miR-144-3p at the binding site of LINC00174.B: Luciferase reporter gene assay results. The presence of ** indicates a comparison with miR-NC. C: Immunoprecipitation was performed using an anti-Ago2 antibody in the RIP assay. **indicates a comparison with the group that received anti-IgG antibodies. D: Expression levels of miR-144-3p in various tissues. E: The cellular expression of miR-144-3p. **signifies the comparison with HIOEC cells. F: The correlation between the levels of LINC00174 and miR-144-3p in SCC-9 cells was examined. WT: LINC00174-WT, and MUT: LINC00174-MUT. **P<0.01

NC group. Furthermore, Bax and E-cadherin were prominently increased, whereas Bcl-2, Vimentin, and Snail showed a notable decrease at the protein levels (P<0.01). The results suggest that the suppression of LINC00174 led to cell apoptosis and triggered EMT. The inhibitor group displayed notable enhancements in cell proliferation, invasion, colony formation, and migration abilities in comparison with the inhibitor-NC group. Furthermore, the inhibitor group exhibited inhibited apoptosis and EMT (P<0.01). Nevertheless, the aforementioned markers exhibited no notable disparities among the si-Inc + inhibitor, si-NC, and inhibitor-NC cohorts (Fig. 5B-F).

MiR-144-3p Targeted Nrf2 in the Downstream Region

It was identified by the bioinformatics tool miRDB (http//mirdb.org/) that miR-144-3p served as a downstream target of Nrf2 mRNA. Furthermore, a distinct binding region was detected between Nrf2 3'-UTR and miR-144-3p (Fig. 6A). It was illustrated in Fig. 6B that the luciferase activity of SCC-9 cells undergoing miR-144-3p mimic and Nrf2 3'-UTR-WT transfection showed a notable reduction by contrast to that of miR-NC-transfected cells (P<0.01). Nevertheless, the luciferase function remained unaltered in the cells that were trans-

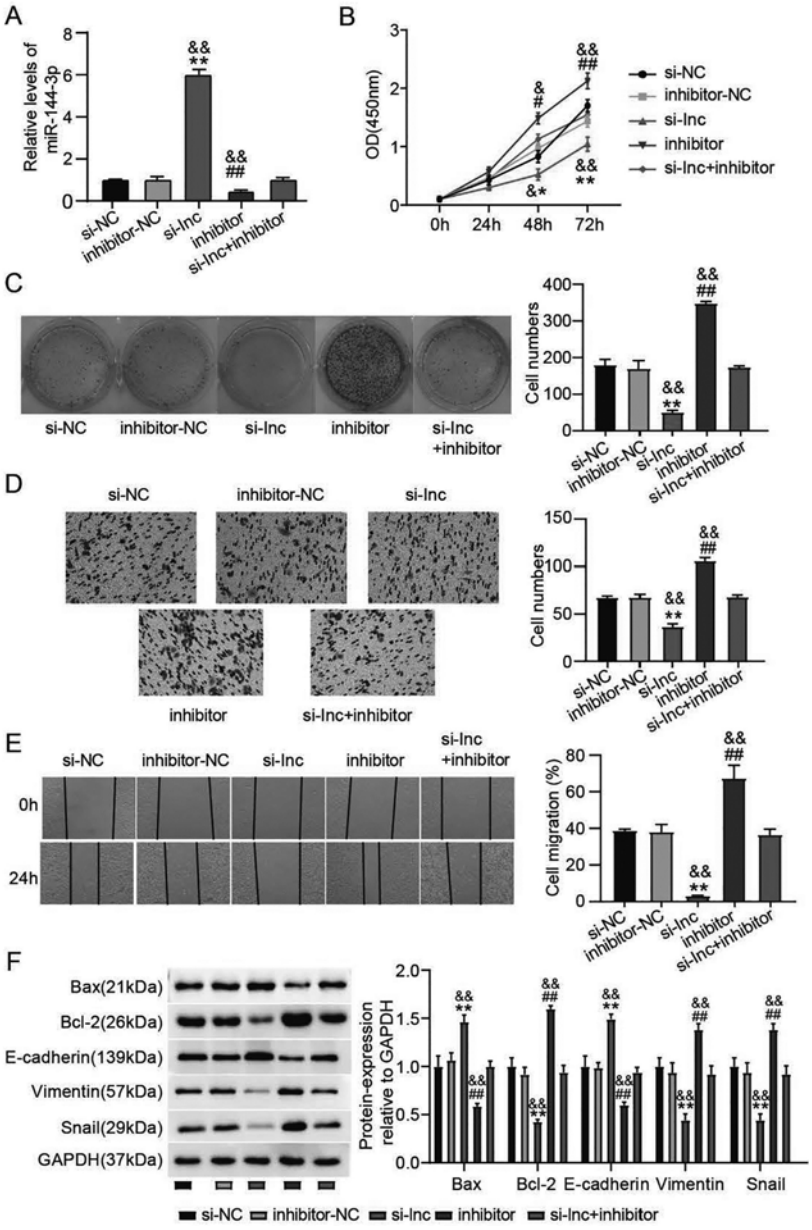

Fig. 5. Blocking miR-144-3p can nullify the impact of LINC00174 suppression on SCC-9 cells. A: Expression of MiR-144-3p observed in SCC-9 cells. B: Cell viability was assessed using the CCK-8 assay. C: Cell colony formation rate. D: Cell invasion capability observed using the Transwell assay. E: The ability of cells to migrate was assessed using a wound healing assay. F: Western blotting detected the protein expressions of Bax, Bcl-2, E-cadherin, Vimentin, and Snail.si-Inc si-LINC00174, as well as miR-144-3p-inhibitor. The symbol * represents comparison with the si-NC group, # represents comparison with the inhibitor-NC group, and represents comparison with the si-Inc + inhibitor group

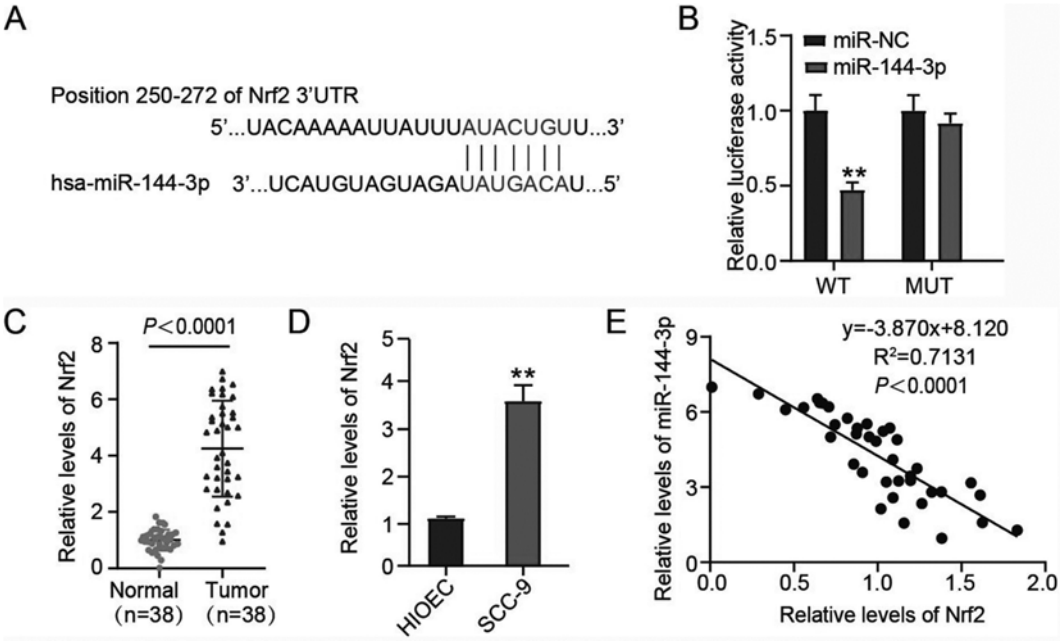

Fig. 6. miR-144-3p targeted gene Nrf2 in the downstream. A: A diagram illustrating the target sequence of Nrf2 at the binding site for miR-144-3p. B: Luciferase reporter gene assay results. *signifies a comparison with miR-NC. C: Expression of the transcription factor Nrf2 in various tissues. D: Nrf2 expression in cells. *signifies the comparison with HIOEC cells. E: The relationship between the expression of Nrf2 and miR-144-3p. WT: Nrf2 3'-UTR-WT, and MUT: Nrf2 3'-UTR-MUT. **P<0.01

fected with Nrf2 3'-UTR-MUT, miR-144-3p imitator, or miR-NC. In addition, OTSCC tissues and cells presented significantly higher Nrf2 levels than normal tongue tissues and cells (Fig. 6C and D). In Figure 6E, miR-144-3p expression was negatively associated with Nrf2 in OTSCC tissues.

Repressing miR-144-3p Counteracted the Impact of Nrf2 Silencing on SCC-9 Cells

The transfection process involved the use of si-NC, inhibitor, inhibitor-NC, si-Nrf2 + inhibitor, and si-Nrf2 on SCC-9 cells. In the si-Nrf2 group, the Western blotting results demonstrated a noteworthy reduction in the expression of Nrf2 protein, while the inhibitor group exhibited an elevation (P<0.01). The si-Nrf2 group compared with the si-NC group exhibited a notable reduction in cell migration, proliferation, invasion, and colony formation abilities. Furthermore, E-cadherin plus Bax were raised, whereas Bcl-2, Snail, and Vimentin were reduced at the protein level (P<0.01). These findings indicate that si-Nrf2 promotes cell apoptosis and induces EMT, which can be reversed by an inhibitor. In addition, the group treated with si-Nrf2 + inhibitor showed no significant differences in terms of propagation, movement, invasion, EMT, and apoptosis compared with the groups treated with si-NC and inhibitor-NC (Fig.7).

DISCUSSION

LncRNAs can sponge miRNAs to suppress their expressions and activities, thereby up-regulating the downstream target genes (Han et al. 2020). This research intended to probe into the effect on OTSCC cell proliferation, invasion, apoptosis, and epithelial-mesenchymal transition exerted by LINC00174 *via* modulating the miR-144-3p/Nrf2 signalling pathway. Both OTSCC tissues and cells were detected with increased LINC00174 expression. Knocking down LINC00174 led to reduced

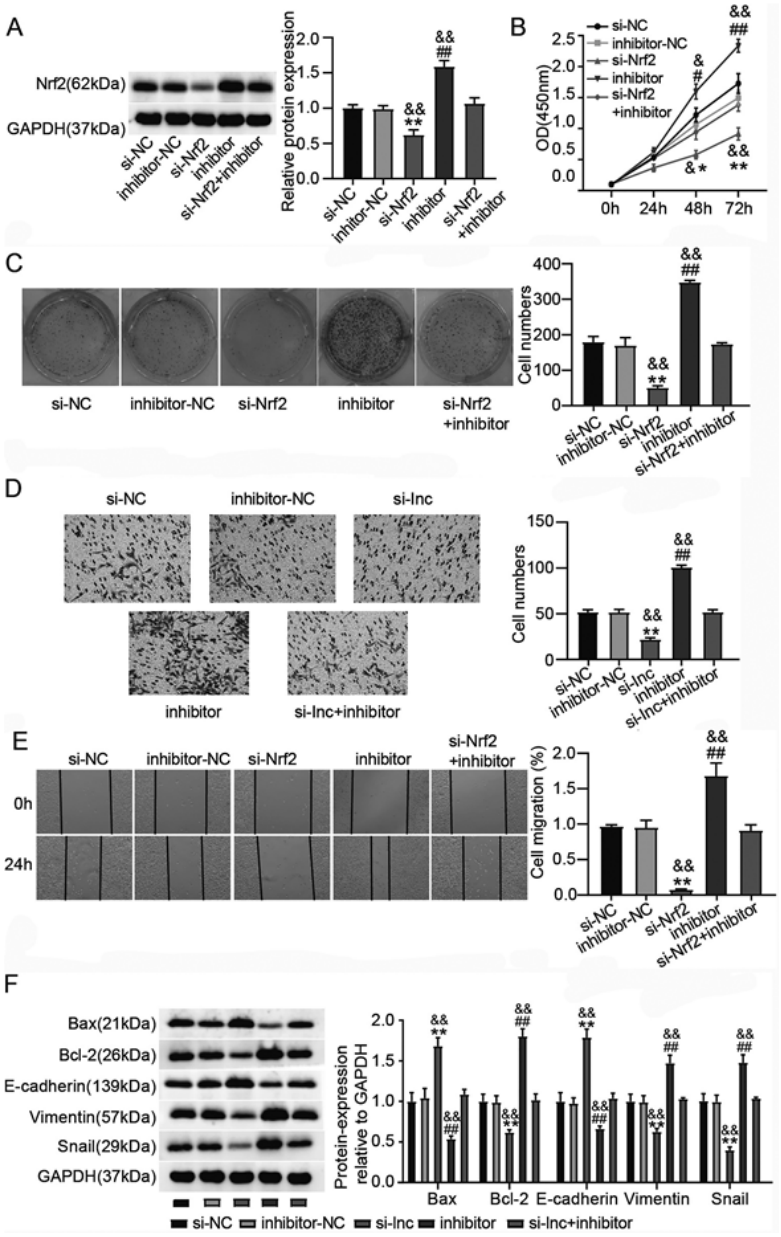

Fig. 7. The elimination of the effect of Nrf2 silencing on SCC-9 cells can be achieved by suppressing miR-144-3p. A: Western blotting detected the protein expression of Nrf2. B: Cell viability was assessed using the CCK-8 assay. C: Cell colony formation rate. D: Cell invasion capability observed using the Transwell assay. E: The ability of cells to migrate was assessed using a wound healing assay. F: Western blotting detected the protein expressions of Bax, Bcl-2, E-cadherin, Vimentin, and Snail.miR-144-3p inhibitor. The symbol * represents comparison with the si-NC group, # represents comparison with the inhibitor-NC group, and represents comparison with the si-Nrf2 + inhibitor group

growth, movement, and infiltration of OTSCC cells, indicating that LINC00174 acts as an oncogenic gene in the progression of OTSCC.

RNAs can be transcribed from about 93 percent of the human genome. Among these transcripts, only 2 percent can be converted into proteins, while the rest translated into lncRNAs (Guglas et al. 2017). LncRNA interference has clear effects on various biological processes and may potentially aid the progress of human cancers (Xie et al. 2018). Park et al. (2022) recently identified approximately 100 types of lncRNAs that control diversified cancers from the aspects of development and advancement. The lncRNAs associated with EMT, cellular migration, and cellular invasion are crucial participants in controlling cancer advancement. In the present study, by silencing LINC00174, SCC-9 cells were inhibited regarding the growth, spread, movement, and EMT, and there was also a decrease in tumour size and weight, indicating the development of OTSCC.

According to Wang et al. (2019), LncRNAs have the ability to counteract the intrinsic impacts of miRNAs on the mRNAs they target. The crucial development of various cancer types is influenced by the ceRNA regulatory network, comprising lncRNA, miRNA, and mRNA. Furthermore, miR-124-3p and other similar miRNAs (Qiao et al. 2020). In 2020, Jiang et al. discovered miR-193-5p, while Chang et al. (2022) identified miR-657-5p. The roles of OTSCC cells' proliferation, metastasis, and EMT regulation have been proven to be vital. In its prediction, starBase v2.0, a bioinformatics software, identified a possible site for LINC00174 to interact with miR-144-3p. Silencing LINC00174 led to miR-144-3p upregulation in SCC-9 cells at the expression level. Additionally, blocking miR-144-3p reversed the effects of LINC00174 suppression, leading to enhanced migration, invasion, and EMT in SCC-9 cells. According to Wu et al. (2019a), miR-144-3p was found to be a cancer inhibitor due to its effects on different cancerous cells in terms of differentiation besides growth. It was uncovered in the present study that SCC-9 cells possessed reduced miR-144-3p expression. LINC00174 expression showed an inverse correlation with this gene, with a role of tumour growth suppressor. Overall, LINC00174 exerted an oncogenic role through restraining miR-144-3p expression.

The involvement of multiple miRNAs, as well as post-translational modifications, transcriptional control, translation, and epigenetic mechanisms, are regulated by Nrf2 (Joo et al. 2019). The entry of Nrf2 induced by ROS into the nucleus can decrease the susceptibility of tumours to radiation treatment while promoting cancerous cell diffusion (Jin et al. 2019). Nrf2 exists at a low expression level in mesenchymal together with epithelial cells, but it is notable in cell phenotypes that exhibit a blend of epithelial and mesenchymal traits. This suggests that elevated Nrf2 levels in cells could trigger EMT (Bocci et al. 2019). As revealed by the miRNA target prediction algorithm, Nrf2 had a binding site for miR-144-3p. MiR-144-3p suppressed Nrf2 expression through conjugating with its 3'-UTR in SCC-9 cells. Moreover, the opposite relation of miR-144-3p expression to Nrf2 in SCC-9 cells was additionally validated by this inquiry. The growth, infiltration, and movement capabilities of SCC-9 cells were significantly hindered by the inhibition of Nrf2, leading to lowered Vimentin and Snail protein levels, increased programmed cell death, and raised E-cadherin protein expression. Moreover, eliminating miR-144-3p manifestation reversed the role of Nrf2 inhibition in repressing SCC-9 cell invasion, movement, and proliferation. Nrf2 existing in cancer cells is able to decrease E-cadherin protein level through an unknown mechanism, ultimately promoting EMT, as reported by Arfmann-Knübel et al. (2015). Furthermore, the stimulation of Nrf2 can diminish cell apoptosis and boost cell growth, whereas suppressing Nrf2 leads to a decline in the levels of Vimentin and Snail expression (Wu et al. 2019b). This study's findings align with those of the literature.

CONCLUSION

In summary, the increased expression of LINC00174 in OTSCC cells stimulates the aggressive traits and EMT via the miR-144-3p/Nrf2 signalling pathway.

RECOMMENDATIONS

In the future, the treatment of OTSCC can rely on the essential preclinical foundation established by the findings of this study.

FUNDING

This study was financially supported by Research Programs of Zhejiang Provincial Department of Education (No. Y202250860) and Science

Foundation of Ningbo Oral Health Research Institute (No. NK20210006; NK20210007).

ABBREVIATIONS

Bax: Bcl-2-associated X;
Bcl-2: B-cell lymphoma-2;
CCK-8: cell counting kit-8;
EMT: epithelial-mesenchymal transition;
FBS: foetal bovine serum;
GAPDH: Glyceraldehyde-3-phosphate dehydrogenase;
HIOEC: human immortalised oral epithelial cell line;
LINC: long non-coding ribonucleic acid;
lncRNA: long non-coding ribonucleic acid;
Nrf2: nuclear factor erythroid 2-related factor 2;
OD: optical density;
OTSCC: oral tongue squamous cell carcinoma;
RIP: RNA immunoprecipitation;
si-NC: small interfering-negative control;
3'-UTR: three prime untranslated region;
WT/MUT: wild-type/mutant.

REFERENCES

Adeoye J, Tan JY, Choi SW et al. 2021. Prediction models applying machine learning to oral cavity cancer outcomes: A systematic review. *Int J Med Inform*, 154: 104557.

Arfmann-Knübel S, Struck B, Genrich G et al. 2015. The crosstalk between Nrf2 and TGF-β1 in the epithelial-mesenchymal transition of pancreatic duct epithelial cells. *PLoS One*, 10: e0132978.

Bocci F, Tripathi SC, Vilchez Mercedes SA et al. 2019. NRF2 activates a partial epithelial-mesenchymal transition and is maximally present in a hybrid epithelial/mesenchymal phenotype. *Integr Biol*, 11: 251-263.

Bray F, Ferlay J, Soerjomataram I et al. 2018. Global cancer statistics 2018: GLOBOCAN estimates of incidence and mortality worldwide for 36 cancers in 185 countries. *CA Cancer J Clin*, 68: 394-424.

Cao HL, Gu MQ, Sun Z et al. 2020. miR-144-3p contributes to the development of thyroid tumors through the PTEN/PI3K/AKT pathway. *Cancer Manag Res*, 12: 9845-9855.

Chang L, Wang D, Kan S et al. 2022. Ginsenoside Rd inhibits migration and invasion of tongue cancer cells through H19/miR-675-5p/CDH1 axis. *J Appl Oral Sci*, 30: e2022 0144.

Cheng X, Sha M, Jiang W et al. 2022. LINC00174 suppresses non-small cell lung cancer progression by up-regulating LATS2 via sponging miR-31-5p. *Cell J*, 24: 140-147.

De Araújo AA, Leite AF, Di Lanaro N et al. 2022. Intra-oral and lower lip squamous cell carcinoma: a comparative analysis of the lymphocytic host response. *Oral Surg Oral Med Oral Pathol Oral Radiol*, 134: e209.

Guglas K, Bogaczyñska M, Kolenda T et al. 2017. lncRNA in HNSCC: Challenges and potential. *Contemp Oncol*, 21: 259-266.

Han TS, Hur K, Cho HS et al. 2020. Epigenetic associations between lncRNA/circRNA and miRNA in hepatocellular carcinoma. *Cancers*, 12: 2622.

Jiang L, He C, Zhang X et al. 2020. MiR-193b-5p inhibits proliferation and enhances radio-sensitivity by down-regulating the AKT/mTOR signaling pathway in tongue cancer. *Transl Cancer Res*, 9: 1851-1860.

Jin M, Wang J, Ji X et al. 2019. MCUR1 facilitates epithelial-mesenchymal transition and metastasis via the mitochondrial calcium dependent ROS/Nrf2/Notch pathway in hepatocellular carcinoma. *J Exp Clin Cancer Res*, 38: 136.

Joo MS, Shin SB, Kim EJ et al. 2019. Nrf2 lncRNA controls cell fate by modulating p53 dependent Nrf2 activation as an miRNA sponge for Plk2 and p21cip1. *FASEB J*, 33: 7953-7969.

Kazmierczak D, Hydbring P 2021. Construction of a full-length 32 UTR reporter system for identification of cell-cycle regulating MicroRNAs. In: *Cell Cycle Oscillators: Methods and Protocols*. Springer, pp. 81-94. DOI: 10.1007/978-1-0716-1538-6_7

Lampropoulou DI, Laschos K, Aravantinos G et al. 2021. Association between homeobox protein transcript antisense intergenic ribonucleic acid genetic polymorphisms and cholangiocarcinoma. *World J Clin Cases*, 9: 1785.

Li B, Xiang W, Qin J et al. 2021a. Co-expression network of long non-coding RNA and mRNA reveals molecular phenotype changes in kidney development of prenatal chlorpyrifos exposure in a mouse model. *Ann Transl Med*, 9: 653.

Li B, Zhao H, Song J et al. 2020. LINC00174 down-regulation decreases chemoresistance to temozolomide in human glioma cells by regulating miR-138-5p/SOX9 axis. *Hum Cell*, 33: 159-174.

Li M, Liu Y, Jiang X et al. 2021b. Inhibition of miR-144-3p exacerbates non-small cell lung cancer progression by targeting CEP55. *Acta Biochim Biophys Sin*, 53: 1398-1407.

Li T, Tang C, Huang Z et al. 2021c. miR-144-3p inhibited the growth, metastasis and epithelial-mesenchymal transition of colorectal adenocarcinoma by targeting ZEB1/2. *Aging*, 13: 17349-17369.

Liu M, Liu Q, Fan S et al. 2021. LncRNA LTSCCAT promotes tongue squamous cell carcinoma metastasis via targeting the miR-103a-2-5p/SMYD3/TWIST1 axis. *Cell Death Dis*, 12: 144.

Ma Y, Li Y, Tang Y et al. 2021. LINC00174 facilitates proliferation and migration of colorectal cancer cells via MiR-3127-5p/E2F7 axis. *J Microbiol Biotechnol*, 31: 1098-1108.

Mascitti M, Zhurakivska K, Togni L et al. 2020. Addition of the tumour–stroma ratio to the 8th edition American Joint Committee on Cancer staging system improves survival prediction for patients with oral tongue squamous cell carcinoma. *Histopathology*, 77: 810-822.

Mneimneh WS, Xu B, Ghossein C et al. 2021. Clinicopathologic characteristics of young patients with oral squamous cell carcinoma. *Head Neck Pathol*, 15: 1099-1108.

Park EG, Pyo SJ, Cui Y et al. 2022. Tumor immune microenvironment lncRNAs. *Brief Bioinform*, 23: bbab504.

Qiao CY, Qiao TY, Jin H et al. 2020. LncRNA KCNQ1OT1 contributes to the cisplatin resistance of tongue cancer through the KCNQ1OT1/miR-124-3p/TRIM14 axis. *Eur Rev Med Pharmacol Sci*, 24: 200-212.

Wang L, Cho KB, Li Y et al. 2019. Long Noncoding RNA (lncRNA)-mediated competing endogenous RNA networks provide novel potential biomarkers and therapeutic targets for colorectal cancer. *Int J Mol Sci*, 20: 5758.

Wang Z, Wang Q, Bao Z et al. 2020. LINC00174 is a favorable prognostic biomarker in glioblastoma via promoting proliferative phenotype. *Cancer Biomark*, 28: 421-427.

Wu J, Zhao Y, Li F et al. 2019a. MiR-144-3p: A novel tumor suppressor targeting MAPK6 in cervical cancer. *J Physiol Biochem*, 75: 143-152.

Wu S, Lu H, Bai Y 2019b. Nrf2 in cancers: A double edged sword. *Cancer Med*, 8: 2252-2267.

Xie S, Yu X, Li Y et al. 2018. Upregulation of lncRNA ADAMTS9-AS2 promotes salivary adenoid cystic carcinoma metastasis via PI3K/Akt and MEK/Erk signaling. *Mol Ther*, 26: 2766-2778.

Zhao S, Chen W, Li W et al. 2021. LncRNA TUG1 attenuates ischaemia-reperfusion-induced apoptosis of renal tubular epithelial cells by sponging miR-144-3p via targeting Nrf2. *J Cell Mol Med*, 25: 9767-9783.

Paper received for publication in February, 2023
Paper accepted for publication in November, 2023